Robert W. Pease
David A. Nichols
University of California
Riverside, CA 92502

Energy Balance Maps from Remotely Sensed Imagery

Isarithmic maps showing urban heat islands, surface albedos, energy absorbed by the surface, and net radiation were constructed from scanner data acquired over Baltimore.

Introduction

Calibration and constant gain are properties which have rendered electro-optical scanners essentially imaging radiometers. The simultaneous imaging of shortwave solar and longwave thermal spectral bands has made possible synoptic maps showing the spatial diversity of various energy-related phenomena as complex as the radiation balance at the terrestrial surface known as net radiation.

rough surfaces of an urban business district present thermal cavity structures the environmental effects of which cannot be accurately assessed from observations at ground level or within the cavity structure itself. Calibrated multispectral scanners on airborne or satellite platforms acquire data from above, rather than in, urban and other terrain and make possible the display of the spatial diversity of these energy-related phenomena in synoptic map form.

Abstract: *Synoptic maps showing the spatial distributions of energy-related phenomena over the terrestrial surface have not been feasible with traditional instruments and observation techniques. The advent of calibrated multispectral optical scanners, however, has made possible the rapid measurement of surface energy emittance and reflectance. Data acquired in a few minutes with scanners from airborne platforms can be translated into maps showing urban heat islands, surface albedos, energy absorbed by the surface, and net radiation. An experiment using the ERIM M-7 scanner, and Baltimore as a test-site city, has successfully yielded isarithmic maps of these phenomena as they existed during an imaging overflight. Methods for acquiring calibrated data from a scanner and the construction of maps from image transparencies are described and evaluated.*

Surface energy-exchange phenomena have become important aspects of climatological research. Much of the effort to date has been involved with analysis of energy budgets for relatively few specific points, however, because of the elaborate and costly nature of ground radiation measuring arrays. Cost and observational time constraints have prevented a synoptic spatial view which truly relates the thermodynamic processes taking place. As an example, the

Map displays from scanner imagery require not only the smoothing or generalization of data points but, for complex phenomena such as net radiation, the combination of data from two or more multispectral bands as well. In the project described, this manipulation must be repeated for each data cell in several large matrices. The assistance of a computer, therefore, avoids the extensive and tedious amount of bit-by-bit mathematical manipulation and decision making

Photogrammetric Engineering and Remote Sensing,
Vol. 42, No. 11, November 1976, pp. 1367-1373.

that would be required by manual reduction of data to a map. This paper, then, is not only concerned with the use of scanner data for making maps of surface energy-exchange phenomena but also reports successful attempts to do so by automated means. Without automation, construction of the maps described would not be feasible except in small experimental instances. In the following sections, the maps and their scanner requirements are described first, followed by methods used in the map constructions.

The original imaging for data and the ensuing development of mapping techniques have been sponsored by the Geography Program of the United States Geological Survey in conjunction with studies of the Central Atlantic Regional Test Site (CARETS). Funding for the aerial imaging was provided directly by NASA.

The Maps

Four maps show the synoptic distributions of several energy-related surface phenomena for a flightpath from the northwest to the southeast across Baltimore, Maryland (Figure 1). The data for map construction were generated close to 1345 (1:45 PM) EDT on May 11, 1972, with the aircraft flying at 1,526 metres (5,000 feet) altitude. The image (Figure 1a) is that of the visual red band (0.62–0.70 μm) and has been included to provide geographical orientation for the maps. On the left hand (NW) end is the central business district (CBD) with downtown Patterson Park the prominent rectangular dark area. To the southeast, an industrial area with large-roofed structures, parking lots, rail lines, and tank farms separates the CBD from a residential area that extends to an arm of the Patapsco River estuary. Across the estuary at the southeast end of the flightpath is Sparrows Point steel mill. In all, a considerable variety of urban surface types is represented. The image is one of the three used to provide data for the maps. The other two are that for the near infrared (1.0–1.4 μm) and that for the thermal infrared (9.8–11.7 μm).

Data for specific maps were derived from scanner outputs as follows. The first map (Figure 1b) shows energy emitted by the surface and used data from only the thermal infrared (TIR) channel. For calibration of this channel to surface targets, the radiation temperatures of the target surfaces were measured with a Barnes PRT-5 radiation thermometer with a 10 to 12 micrometre spectral sensitivity. Radiation temperatures relate to the Stefan-Boltzmann equation when the emissivity of the radiating surface is considered unity and are the temperatures derived in this experiment rather than sensible or kinetic temperatures. For this reason, only when longwave energy is absorbed by the surface is emissivity of any concern to the inquiry. The use of radiation temperatures is an intermediate step in the calculation of radiant emittance. By definition this temperature form implies the total energy in a black body curve whereas energy through a spectrally narrow instrument window may not follow the fourth power law. Longwave radiometers, therefore, are typically calibrated in radiation temperatures.

The map of albedos (Figure 1c) required the combination of images made with visual red and near infrared, weighted as will subsequently be described. The map of energy absorbed by the surface (Figure 1d) uses the unity-complement of the albedo as a multiplicative modifier of ground-measured solar radiation (both beam and diffuse) to ascertain the solar energy absorbed. To this is added absorbed downwelling longwave atmospheric radiation. Although we are here primarily concerned with radiation temperatures, an emissivity must be assumed to assess that portion of the longwave radiation which enters the surface energy budget. For most terrestrial surfaces, the emissivities for wavelengths close to 10 micrometres range from 0.90 to 0.98, and an average value of 0.95 has been used for longwave absorption. The map of net radiation (Figure 1e) represents the subtraction of values of energy emitted from values of energy absorbed.

In brief, whereas the map of albedos requires only the combination of data from two spectral channels, that for energy absorbed requires the use of the same two channels plus the ground-truth data measured at the surface. The map of net radiation, on the other hand, requires data from three channels to be combined in data cells along with data from surface observations. The ways by which the data from the multiple channels have been combined and ways by which congruency of data cells from more than one spectral image has been maintained are treated in detail in the following section.

Before the explanation of the map construction methods, it should be noted that no attempt has been made to remove the scale distortions inherent in straight scanline geometry. The transverse scale factor is a nonlinear 0.79 to a flightpath scale of 1.00. This error is inverse to the nonlinearity of the

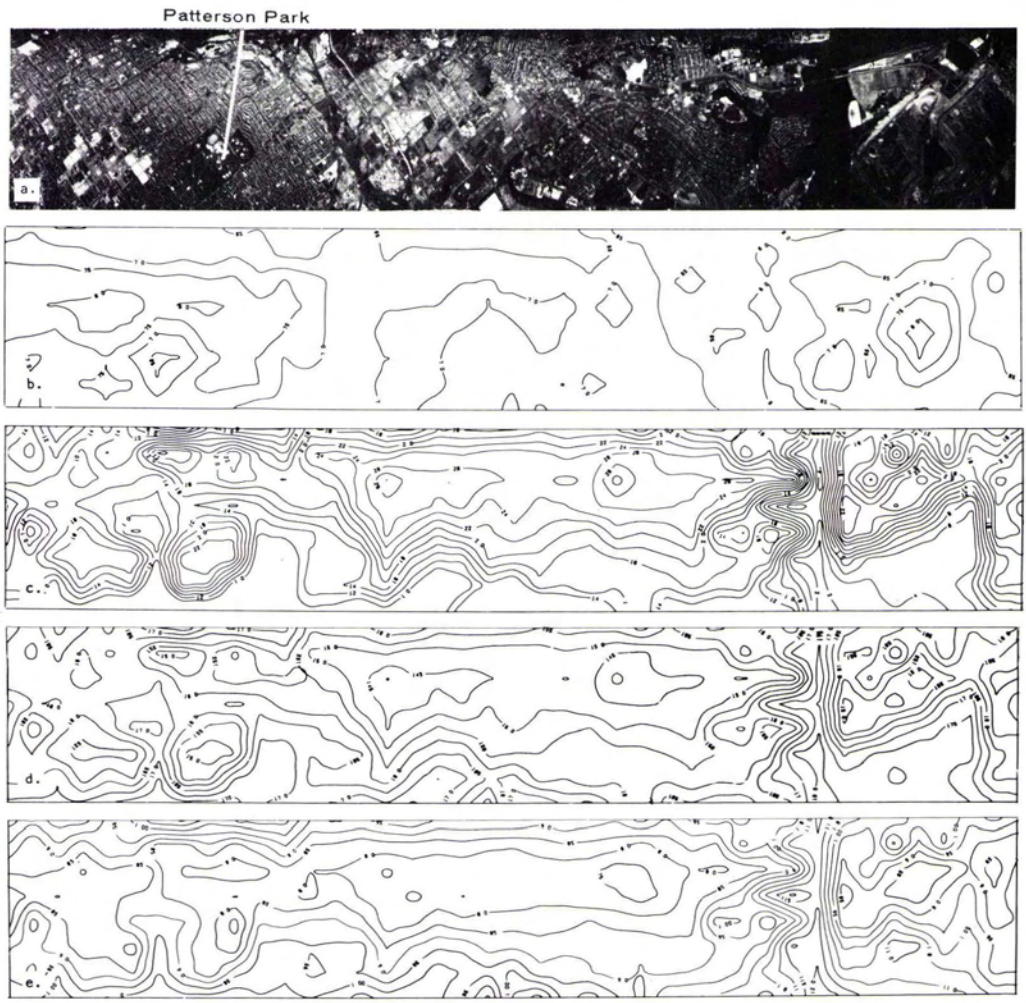

FIG. 1. A sequence of isarithmic maps showing various energy-related phenomena for a flightpath NW–SE across Baltimore, Maryland, at 1345 EDT on May 11, 1972. The image of the visual red band (a) shows the diversity of urban surfaces mapped. The maps generalize (b) the energy being emitted by the surface in langleys/minute × 100, (c) surface albedos in percentages, (d) the energy being absorbed by the surface (ly/min. × 100), and (e) the balance of energy flows at the surface, or net radiation (ly/min. × 100).

tangent functions produced as the optical path swings with constant angular velocity away from nadir.

METHODS USED IN MAP CONSTRUCTION

Requisites for making surface energy-exchange maps from imaged data are: (1) the multispectral scanner must have constant gain and internal calibration sources are desirable, (2) the scanner must be calibrated to the terrestrial surface for the spectral bands or channels from which the map-making data are to be taken, (3) data from both a thermal infrared channel and short-wave (solar wavelengths) channels appropriate for albedo determination must be available, (4) data must be entered into the processing system in such a manner that values from several spectral bands will be for congruent surface areas, and (5) data points must be smoothed or averaged to permit the simplification inherent in map displays.

There are two ways for calibrating a constant gain scanner to the surface. That employed in this study is by the use of calibration targets, areas of homogeneous surface

large enough to yield image elements that can be measured densitometrically. Several targets were chosen to give a range in both temperature and reflectance values. The use of target calibration automatically compensates for any effects that the atmosphere in the optical path may have on the surface signal.

The second method applies only to the terrestrially emitted or longwave TIR spectral band. For this, a relatively simple gray-window model can be constructed which involves the attenuation of the surface-emitted signal by the intervening water vapor, turbidity, and pollution in the optical path while at the same time these absorbing elements are by their own emission adding strength to the attenuated surface signal (Pease, 1971). Current processing of Skylab data, where no calibration targets are available, uses the gray-window approach (Jenner *et al.*, 1976), but targets were available and used for the Baltimore experiment.

The day of the imaging flight was cool and clear following the passage of a cold front the previous night. Relatively dry air minimized the modification of the TIR signal in the 9.8–11.7 μm spectral sensing band. Although the transmissivity of the relatively dry air was 0.90 (surface to sensor), a small error would have ensued for the surface temperatures of the CBD which were some 20°C above the mean temperature of the air column. The gray-window modification of the surface-emitted signal by the atmosphere cannot be ignored in careful remote temperature measurements through the so-called water vapor window (8.0–12.0 μm) due to residuals of spectrally close water vapor absorption bands. At this time, no satisfactory gray-window model has been created for reflected sunlight and target calibration must be used.

Reduction of data to a map form involves the use of data-averaging cells in a matrix, a form of block smoothing, to achieve the generalization of information a map requires. Data cells can be delineated on photographic transparencies of desired spectral channels or on digitized versions of scanner magnetic tapes. This inquiry extracted data from transparencies. Several types of map formats are available. Data-averaging cells can be printed as graymaps with a line printer or drafted as discrete data cells, in either case according to a value-intervalled hierarchy of map symbols. The method used for the maps of Figure 1, however, places the averaged values at the centroids of each data cell as control points for plotting isarithmic lines. Since each cell is part of a large matrix, numerous control points are available for automated plotting of the lines. The size of the averaging cell used in this study, however, reduced the number of cells in the matrix. This condition favors the use of the isarithmic format because the cells are too large to produce a map with satisfactory detail when they directly outline value polygons on the map. The line-printed data cell approach was carried out by the Environmental Research Institute of Michigan (ERIM) but with smaller cells which necessitated additional smoothing achieved by moving filters which acted directly upon digitized data to reduce spatial noise in the ensuing graymaps (Thomson and Dillman, 1973). The ERIM inquiry was also funded by NASA and the U.S. Geological Survey and was carried out in cooperation with the study reported here.

The flow of data in the construction of the maps is shown in Figure 2. Briefly stated, average transmittances of discrete data cell areas on the transparencies for the several spectral channels first were measured with a custom-fabricated wide aperture densitometer. The punching of these values

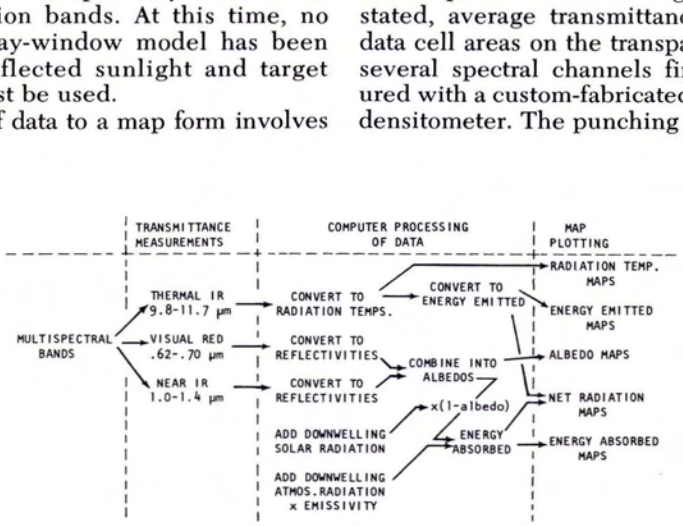

FIG. 2. The flow of data followed in making the maps.

into IBM cards constituted the only manual operations in the map constructions. Each card entry not only contained the average transmittance value for its cell but $x - y$ locational information as to the position of the cell in its larger matrix. Conversion information, previously entered into the computer as sub-routines, operated with appropriate programs to convert transmittances to radiation temperatures (TIR channel) or reflectivities (shortwave channels). The computer created plot tapes for a plotter to automatically draft the maps. An IBM 360-50 computer was used in conjunction with an H. Dell Foster RSS-700 flat-bed vector plotter.

The wide aperture densitometer, with which average transmittances for data cells were measured, is diagrammed in Figure 3. It is a combination of a current-regulated illumination system, a working aperture the size of the data cell on the transparency, and a silicon cell sensor. The sensor actuates a potentiometric recorder mechanism with the voltage developed across the cell load resistor, the latter with a wiper that permits calibration control of the system. The smoothing or averaging aperture chosen was 6.25 mm (0.25 inch) square which gave a ground resolution of 381 metres (1,250 feet). The aperture size determines the degree of block-smoothing of the imaged data. A MacBeth densitometer and its calibrated step-wedge were used to calibrate the custom-fabricated instrument. The measuring components were attached in place of the cursor on an H. Dell Foster $x - y$ digitizer.

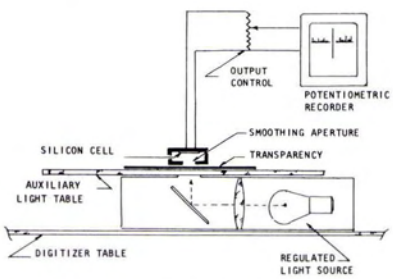

FIG. 3. Diagram of the wide-aperture densitometer used to read transparency transmittances into an automated computer and mapping system. The transparency is attached to a stationary auxiliary light table placed atop an H. Dell Foster $x - y$ digitizer. The light source and sensing cell move with the digitizer cursor arm. Registration in a matrix of averaging data cells is maintained by the digitizing system quantizer.

The preservation of congruency of value areas between the spectral channels of a given flightpath followed in concept a method used successfully in making isarithmic maps of radiation temperatures from data obtained on Barbados during the BOMEX experiment (Pease, 1971). In that instance, a matrix of lines was placed over a transparency image and measurements were made of the discrete cells so delineated. For the current project, cell integrity between spectral bands was maintained by the x and y displays of the quantizer of the digitizer. The separate multispectral images were indexed into the locational system both by image edges and prominent features that appeared on each image. Locational information was punched into the cards automatically each time a transmittance value was entered.

Because all data cell values entered into the automated system were transmittances, of necessity the conversion to energy-related values took place in the computer. An important step in the processing, therefore, was the inclusion of the conversion information previously mentioned. Although scanner measurements recorded initially on magnetic tape are essentially linear, their representation upon a photographic transparency follows the S-shaped sensitometric curve of the photographic film (Figure 4). Because mathematical models of the S-shaped curves proved to be poor fits, the actual graphic conversion curves were simply digitized in their x and y coordinates and then treated in the computer as a series of very short linear equations. The shape of the film sensitometric curve could be determined from the incremental step-wedges along the edges of the transparencies. To make the curves, transmittances of target image elements were measured through the 1 mm aperture of the MacBeth densitometer and plotted against ground-measured surface values.

Conversion information for the TIR channel is shown as the curve in Figure 4a. The target types for which radiation temperatures were recorded at the time of the imaging overflight readily delineate the curve. Conversion information for plotting albedos, however, posed a more complex problem. The work of Dirmhirn (1968) suggests that the "silicon sensitivity" which peaks at 0.8 micrometres provides good measures of albedos due to its distribution of sensitivity above and below the rapid rise in plant (chlorophyll) reflectance that centers at a wavelength of 0.725 micrometres. Reflec-

tance curves for common substances such as soil, blacktop, and concrete, tend to change gradually over the solar wavelengths and therefore their albedos are less prone to error when measured by spectrally selective methods than are those for plant targets. Pease and Pease (1972) have demonstrated that albedo measurement by spectrally selective methods or by spectral samples should be weighted with 60 percent of the sensitivity below the 0.725 micrometre midpoint in the plant reflectance rise and 40 percent above or at longer wavelengths. The two spectral bands used in this study to measure albedos are the visual red (0.62–0.70 μm) for wavelengths shorter than 0.725 micrometres and the near infrared (1.0–1.4 μm) for wavelengths that are longer. Curves converting transmittances to reflectivities for these two sample bands (Figure 4b) were entered as sub-routines and combined with the above 60/40 weighting to yield albedos. Again, congruency of data cells is imperative to accuracy of results.

After all data had been read from the transparencies and punched into cards, a master tape file was prepared. The data, now in machine-compatible form, were subjected to manipulation. For this purpose, two programs were written. The first utilizes sub-routines to convert transmittance data from the TIR channel to radiation temperatures. The second program contains several steps. (1) It determines an albedo by combining the reflectivities of the two sample spectral bands according to the 60/40 weighting. (2) With the factor (1 – albedo), the program converts solar radiation (entered as a constant in the program for this imaging flight) into solar energy absorbed. (3) To this is added the downwelling longwave atmospheric radiation (also a constant program value for this flight) after reduction by the previously explained standard 0.95 emissivity to achieve total energy absorbed by the surface. (4) To determine net radiation, a cell radiation temperature was entered from the first program, converted to langleys per minute with the appropriate form of the Stefan-Boltzmann equation, and added as a negative quantity to energy absorbed as a positive quantity. This sequence of data processing was performed for each data cell in the flightpath matrix. The procedure emphasizes the importance of maintaining perfect registry of data cells between the multispectral bands used. At different stages of processing, maps showing various energy-related surface phenomena were made by applying data values to the centroids of data cells in the matrix and interpolating isarithmic lines.

Although a variety of contouring programs could have been used for drafting the maps on the plotter, that used in this project is the TOPO* program with a pre-processor linear interpolation routine which has the dual purpose of scaling the matrix size and smoothing the surface.

Evaluation of Results

Because the dual technologies of multispectral scanning and automated isoline mapping are not new, it is felt that the important contributions of this project are (1) the successful creation of maps showing

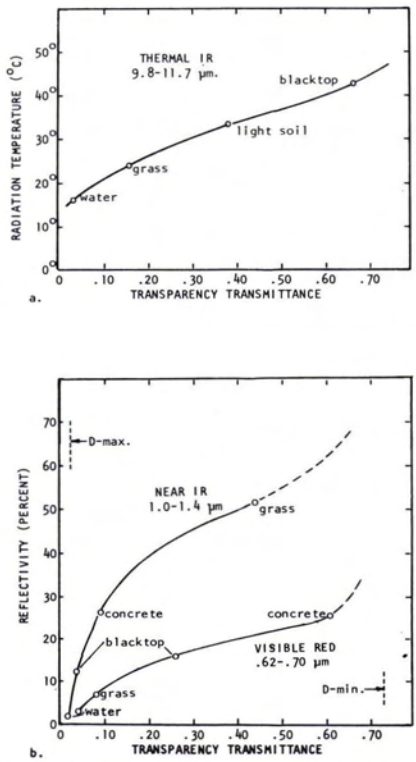

FIG. 4. Curves to convert (a) the thermal infrared image to surface radiation temperatures and (b) two shortwave images to reflectivities which when combined give albedos. Ground calibration targets are indicated. The S-shape matches sensitometric curve of the transparency film.

* The TOPO program was written by Raymond Postma as a part of a land-planning tools software package for the Environmental Systems Research Institute of Redlands, California.

distributions of energy-related surface phenomena other than simple displays of thermal state and (2) the symbiotic integration of scanner and automated cartography techniques to achieve such maps.

As regards accuracy of the maps, the following observations can be made. Radiation temperatures closely correspond to target ground measurements which may not be surprising since these measurements were used to make the conversion curves. Albedo values, less directly derived, agree with the authors' own experience in measuring a variety of surfaces by standard pyranometric methods. Vegetated grass surfaces such as parks, for example, have albedos of 20 to 22 percent which match ground truth measurements and are in a generally accepted range of values for this type of surface (Sellers, 1965; Kondratyev, 1969; Kung, Bryson, and Lenschow, 1964). Net radiation values, which required the most complex series of processing manipulations and thus potentially were most prone to error, also appear reasonable in light of the authors' experience in microclimatology. The ground-measured net radiation of the blacktop surface of one of the prime calibration targets at the time of overflight was 0.81 langleys per minute. On the generalized map of the calibration run (not included), the value at the target location interpolated as 0.77 ly/minute, a low order of error. It should be noted that perfect agreement cannot be obtained between averaged data and point measurements. The value of 1.20 ly/min. over water reflects the latent energy sink of evaporation.

Variations in values entered as constants in the data manipulations could have caused serious errors in the mapped distributions. Incoming solar radiation, for example, might well have varied over the flightpath due to urban pollution, especially that arising from the steel mill. For this reason, a pyranometric reconnaissance to detect diversity in solar input was made over the area at the high sun diurnal period just before the imaging flight. Values varied less than 0.01 ly/min. from the nominal 1.42 ly/min. used in the calculations. In a like manner, the nature of the airmass was conducive to spatially homogeneous distribution of atmospheric down radiation. The ideal conditions of the imaging day, however, do not rule out the necessity for ascertaining possible inconsistencies in ground-measured energy inputs.

Regarding the utility of the maps, one purpose is to supply spatially comparable data to be used in modeling in such areas as urban planning and the new field of land use climatology. Possibilities in this direction are still to be explored, but certain facts are already apparent. For example, albedo appears to be the factor controlling net radiation which is often considered a broad measure of the injection of natural energy into a terrestrial thermal system. Due to relatively high albedos, parks in an urban business district appear as poor absorbers of solar energy. They may seem cool, therefore, for reasons other than their being latent energy sinks, the commonly held cause. Other examples could be cited.

Current experience with Skylab S-192 data is advancing techniques herein described. Use of the gray-window model is being advanced to eliminate the need for calibration targets for thermal mapping. The utility of satellite platforms for acquiring data to make surface energy-exchange maps has been tentatively proved (Jenner, *et al.*, 1976).

Future energy-exchange mapping with the aid of multispectral scanners depends to a great extent upon the availability of appropriate data. The forthcoming Heat Capacity Mapping Mission (HCMM) could well provide more satellite data with a thermal infrared channel and the necessary calibration capability. Use of a high-flying aircraft as a scanner platform should be considered as a compromise between the low-flying aircraft used in this project with its narrow scan path and expensive satellite platforms. A scanner at 20,000 metres (65,500 feet) would provide an intermediate spatial coverage with greater detail than the satellite and could be used at specific times which best fit observational needs. Although future instrument platforms are not well defined at this time, it can be assumed that, if synoptic maps of surface energy-related phenomena are of value, the necessary scanner data will be forthcoming.

References

Dirmhirn, Inge, 1968, "On the Use of Silicon Cells in Meteorological Radiation Studies," *Journal of Applied Meteorology*, Vol. 7, pp. 702–707.

Jenner, C. B., J. E. Lewis, S. I. Outcalt, and R. W. Pease, 1976, "Land Use Climatology . . . ," Chapter 3 of R. H. Alexander *et al., Applications of Skylab Data to Land Use and Climatological Analysis*, U.S. Geological Survey/Geography Program, Final Report Skylab/EREP Investigation No. 469.

Kondratyev, K. Ya., 1969, *Radiation in the Atmosphere*, Academic Press, New York.

Kung, E. C., R. A. Bryson, and D. H. Lenschow, 1964, "Study of a Continental Surface Albedo on the Basis of Flight Measurements and Structure of the Earth's Surface Cover over North America," *Monthly Weather Review*, Vol. 92, No. 12, pp. 543–564.

Pease, R. W., 1971, "Mapping Terrestrial Radiation Emission with a Scanning Radiometer," *Proceedings of the Seventh International Symposium on Remote Sensing of Environment*, Vol. 1, pp. 501–510, University of Michigan, Ann Arbor.

Pease, S. R. and R. W. Pease, 1972, *Photographic Films as Remote Sensors for Measuring Albedos of Terrestrial Surfaces*, Technical Report V, U.S. Geological Survey Contract 14-08-0001-11914.

Sellers, W. D., 1965, *Physical Climatology*, University of Chicago Press, Chicago.

Thomson, F. J. and R. D. Dillman, 1973, *Baltimore Maryland Radiation Balance Mapping*, Technical Report, Environmental Research Institute of Michigan (unpublished).

Errata

In the article "Applied Photo Interpretation for Airbrush Cartography" by Jay L. Inge and Patricia M. Bridges in the June 1976 issue Figures 1a and 1c (page 751) have been interchanged; and the sentence beginning on the fourth line, first column on page 754 should read "The horizontally high-pass filtered version (Figure 1a) and the vertically high-pass version (Figure 1b) depress surface coloration and enhance high frequency contrast."

In the July 1976 Yearbook issue the winners of the Autometric Award for the last five years (page 962) should read

1972—*Dr. Edward Yost* and *Sondra Wenderoth*
1973—*Kenneth R. Piech* and *John E. Walker*
1974—*M. R. Specht, N. L. Fritz,* and *D. Needler*
1975—*Kalman N. Vizy*
1976—*Dr. Robert G. Reeves*

The July 1976 Yearbook issue failed to list the following Emeritus Members (page 966):

Ray Anderson	*Pliny Gale*	*Gilbert B. Miller*
Gen. Benjamin Arcoverde	*Douglas E. Henriques*	*William H. Moorhouse*
Stanley B. Ash	*Jack J. Ingram*	*Richard B. Soloman*

If other names were left out, please inform the Society.

In the article "The Brock Brothers and the Brock Process" by Harry Tubis in the August 1976 issue, the first line, second column of page 1029 should read "(Figures 3 and 4).", and the first sentence of the last paragraph in the first column on page 1032 should begin "This completes . . .".

In the article "Compilation Base Orientation by Graticule" by Richard H. Duncan in the September 1976 issue, the 14th to the 6th lines from the bottom in the left-hand column of page 1158 should be removed; the 16th line in the right-hand column of page 1158 should read "X_g, Y_g, and E_g of points . . ."; the second of the three equations toward the bottom of the right-hand column of page 1158 should read

$$Y_{mdc} = b_1X_g + b_2Y_g + b_3X_g^2 + b_4X_gY_g + b_5Y_g^2 + b_6X_g^3 + b_7X_g^2Y_g + b_8X_gY_g^2 + b_9Y_g^3;$$

and the second reference at the end of the article should read "Bendix Research Laboratories, *Handbook for AS-11B-1 Automated Analytical Stereoplotters*, Vol. 1, December 1969."

Cover Photos Needed

Photographs suitable for the cover of *Photogrammetric Engineering and Remote Sensing* are needed. Either black-and-white or color may be used; however, because color reproduction is costly, we request that the donors of color material if at all possible cover the additional cost (approximately $750). Please submit cover material to the Editor, American Society of Photogrammetry, 105 N. Virginia Ave., Falls Church, VA 22046.